NASA
Technical Memorandum 107284

Army Research Laboratory
Memorandum Report ARL–MR–152

Three-Dimensional Navier-Stokes Analysis and Redesign of an Imbedded Bellmouth Nozzle in a Turbine Cascade Inlet Section

P.W. Giel and J.R. Sirbaugh
NYMA, Inc.
Brook Park, Ohio

I. Lopez
Vehicle Propulsion Directorate
U.S. Army Research Laboratory
Lewis Research Center
Cleveland, Ohio

G. J. Van Fossen
Lewis Research Center
Cleveland, Ohio

Prepared for the
39th International Gas Turbine and Aeroengine Congress and Exposition
sponsored by the American Society of Mechanical Engineers
The Hague, Netherlands, June 13–16, 1994

National Aeronautics and
Space Administration

Three-Dimensional Navier-Stokes Analysis and Redesign of an Imbedded Bellmouth Nozzle in a Turbine Cascade Inlet Section

P. W. Giel and J. R. Sirbaugh
NYMA, Inc.
NASA Lewis Research Center
Brook Park, OH 44142

I. Lopez
U.S. Army Research Laboratory
Vehicle Propulsion Directorate
Lewis Research Center
Cleveland, OH 44135

G. J. Van Fossen
NASA Lewis Research Center
Internal Fluid Mechanics Division
Cleveland, OH 44135

ABSTRACT

Experimental measurements in the inlet of a transonic turbine blade cascade showed unacceptable pitchwise flow non-uniformity. A three-dimensional, Navier-Stokes computational fluid dynamics (CFD) analysis of the imbedded bellmouth inlet in the facility was performed to identify and eliminate the source of the flow non-uniformity. The blockage and acceleration effects of the blades were accounted for by specifying a periodic static pressure exit condition interpolated from a separate three-dimensional Navier-Stokes CFD solution of flow around a single blade in an infinite cascade. Calculations of the original inlet geometry showed total pressure loss regions consistent in strength and location to experimental measurements. The results indicate that the distortions were caused by a pair of streamwise vortices that originated as a result of the interaction of the flow with the imbedded bellmouth. Computations were performed for an inlet geometry which eliminated the imbedded bellmouth by bridging the region between it and the upstream wall. This analysis indicated that eliminating the imbedded bellmouth nozzle also eliminates the pair of vortices, resulting in a flow with much greater pitchwise uniformity. Measurements taken with an installed redesigned inlet verify that the flow non-uniformity has indeed been eliminated.

List of Symbols

- C_x - blade axial chord, $C_x = 12.70$ cm (5.000 in.)
- C_p - total pressure coefficient, $C_p = (P' - P_{in})/(P'_{in} - P_{in})$
- M - Mach number
- P - pressure
- Re_x - Reynolds number, $Re = \rho u_{in}\, x/\mu$
- s - blade and inlet section span, $s = 15.24$ cm (6.000 in.)
- T - temperature
- u - velocity in x-direction
- v - velocity in y-direction
- w - velocity in z-direction
- x - axial direction, nondimensionalized by span, s
- y - pitchwise direction, nondimensionalized by span, s
- y' - pitchwise direction parallel to blade leading edges, nondimensionalized by span, s
- y^+ - normalized distance in inner coordinates
- z - spanwise direction, nondimensionalized by span, s
- α - inlet flow angle to blade row
- δ - boundary layer thickness
- μ - dynamic viscosity
- ρ - density
- ω - nondimensional vorticity

Subscripts

- *in* - freestream inlet value
- *ex* - freestream exit value

Superscripts

- ' - total conditions

1. INTRODUCTION

As the dependence on computational fluid dynamics and heat transfer increases in the design and analysis of turbomachinery, the need for detailed, benchmark quality experimental data also increases. This data is required for validation of codes and models as well as for determination of model functions and constants. As such, one requirement of a benchmark experiment is that more uniform, better documented, and generally higher quality inlet flow is needed. The results of a CFD calculation can be only as good as the boundary conditions, particularly the inlet conditions, that are applied to it. The importance of the inlet geometry and inlet conditions was pointed out in an experimental study by Kiock et al. (1985) where the same blade shape was examined in four wind tunnels and it was shown that only two of the tunnels exhibited two-dimensional inlet flow. An AGARD report on test cases for computation of internal flows in aero engine components (see Fottner, 1990) also stresses the importance of clearly defined upstream flow conditions.

A new Transonic Turbine Blade Cascade Facility was designed and built at the NASA Lewis Research Center to study the flow and heat transfer characteristics of advanced turbine blades. The intent of the cascade is to provide benchmark quality data for CFD code and model verification. Initial measurements of the flow upstream of the cascade, however, indicated that uniform inlet flow had not been achieved.

CFD was itself a tool available to help determine the source of the non-uniformity and then to help eliminate it. The details of several calculations and the results obtained from those calculations will be described. The first calculation was run as an analysis of the original geometry to determine the source of the non-uniform flow. As the results will show, the cavity formed by an imbedded bellmouth inlet appeared to be the source. The next calculation was performed to determine if bridging the region between the bellmouth and the

upstream wall would eliminate the problem. A third and final calculation was performed to ensure that the upstream region of the facility did not contribute an additional source of flow non-uniformity. Each of these three computations are described separately below. Finally, experimental measurements taken with the modified inlet geometry will be presented and compared to the calculations.

The analysis was not performed during the initial design for several reasons. As is the case of the design of any new facility, the bellmouth inlet was just one of several potential problems -- all others appear to have turned out well. In the course of the initial design, an inlet analysis with the degree of intensiveness that will be shown to be necessary would have been difficult to justify. Also, the inlet design was based somewhat on another turbine cascade facility with a shorter inlet section that performed well (see Stabe and Kline, 1974 and Kline, Moffitt, and Stabe, 1983). Other similar inlet geometries can be found in the literature (see Meauze, 1979).

2. DESCRIPTION OF FACILITY

The design of new experimental research facilities involves compromises and the use of novel, but often untested designs. A new Transonic Turbine Blade Cascade Facility was designed and built at the NASA Lewis Research Center to study the flow and heat transfer characteristics of advanced turbine blades. Some noteworthy features of the facility are its ability to achieve transonic Mach numbers, its high blade count for periodicity, and its large scale, which facilitates detailed flow and heat transfer measurements. Also, because of its large scale and transonic flow conditions, realistic engine Reynolds numbers are achieved with an inlet pressure near one atmosphere. An overall view of the cascade facility is shown in Figure 1. Dimensions relevant to the work presented here are included in the figure, but a more detailed description is given by Verhoff, Camperchioli, and Lopez (1992).

The blade shape is typical of a high pressure turbine rotor. A highly three-dimensional flow field was sought in the blade passages, characteristic of an actual gas turbine environment. To obtain this highly 3-D flow field, a thick inlet boundary layer was desired at the face of the blade row. A 4.5 meter long inlet section was used to develop this thick inlet boundary layer. At the same time, the capability to examine off-design incidence angle variations or to allow for blades of different inlet incidence was desired. The incidence can vary over a range of + 15° to − 30° from the design condition (note that Figure 1 shows the blade row set at the design inlet flow angle, $\alpha = 63.64°$). This incidence variation capability was achieved by allowing the blade row, mounted on a circular disk, to rotate about its center passage. As the blade row is rotated for off-design incidence angles, its upper end is hinged to the upper inlet board, and its lower end slides along the lower inlet board, thus changing the vertical and horizontal positions of the downstream ends of both boards. The upstream ends of the inlet boards are then adjusted vertically, so that the boards remain parallel to each other, and horizontally, so that the inlet board leading edges are at equal x locations. To satisfy all of these desired capabilities, a compromise was reached with the inlet boards, allowing their leading edges to form imbedded bellmouth nozzles.

The idea of a bellmouth nozzle with moveable inlet boards was borrowed from another turbine cascade rig at NASA Lewis (see Stabe and Kline (1974) and Kline, Moffitt, and Stabe (1983)). The bellmouth nozzle described in these reports also formed cavities like those of the present study shown in Fig. 1. However, that cascade had a very short inlet section compared to the one in the present study and its inlet was open to the atmosphere. Other similar geometries can also be found in the literature; see, for example, Meauze (1979). The bellmouth nozzle and cavity geometry is also very common in solid rocket nozzles, except that their geometry is typically axisymmetric. The bellmouth nozzle created cavities in the inlet of the present study that were somewhat questionable, but the previous experiences mentioned above indicated that they should not have a detrimental effect.

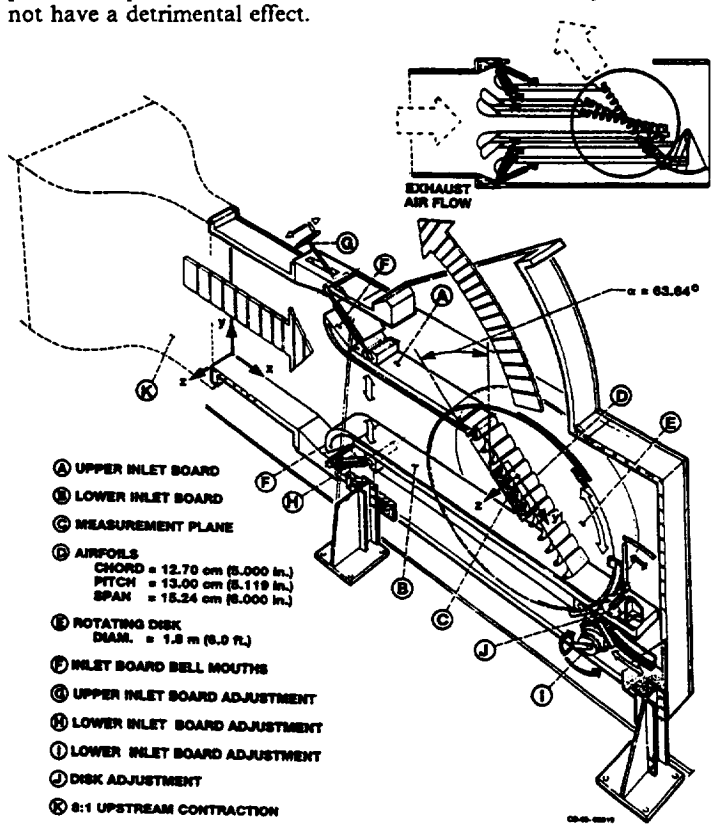

Figure 1. Overall View of Transonic Turbine Blade Cascade Test Section.

The most critical requirement of any cascade inlet section is that it should provide pitchwise periodic, two-dimensional flow upstream of at least three of the center blade passages. To experimentally verify the inlet periodicity, total pressure measurements were taken in a plane 2.2 cm (0.18 C_x) upstream of the blade's leading edges, traversing slightly more than three blade passages. (The measurement plane is shown in Fig. 1). Because a five-hole probe was used for the measurements, the first data point in the spanwise direction was taken 0.635 cm (0.250 inches) from the endwall. Flat-plate boundary-layer correlations indicated that the full boundary-layer thickness, δ, should be approximately 4.25 cm ($\simeq 0.28 \times$ span) in this region. The experimental measurements of total pressure coefficient are shown below in Figure 2. The measurements clearly show that periodic flow had not been achieved. The objective of the present work was to identify the source of the flow non-uniformity and then to propose a design change that would eliminate it.

$$\text{Total Pressure Coefficient, } C_p = \frac{P' - P_{in}}{P'_{in} - P_{in}}$$

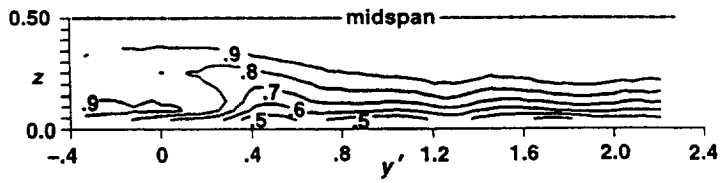

Figure 2. Experimental Measurements of Total Pressure Coefficient in the Original Geometry.

A computational analysis was chosen for several reasons. First, physical accessibility to the inlet section was limited, making flow measurements more than a few chords upstream of the blade's leading edges very difficult. The computational analysis also allows for a better understanding of the physics than a set of discrete measurements might because the flow properties can be analyzed throughout the entire domain. This understanding can give great insight when proposing design changes. The computational approach also enables design changes to be examined cheaper and more quickly than an experimental approach would.

3. COMPUTATIONAL METHODS AND MODELS

3.1. Code Description

The PARC CFD code that was used in this study solves the Reynolds averaged Navier-Stokes equations formulated in the strong conservation law form for a curvilinear coordinate system according to the method described in *PARC Code: Theory and Usage* (Cooper and Sirbaugh, 1989). The viscous flux terms are handled explicitly on the right-hand side of the equations. The inviscid flux terms are time-linearized, resulting in an explicit flux term on the right-hand side and an additional left-hand side term. Second order accurate central differencing is used to calculate the inviscid fluxes. Since the flux terms are modeled using central differences, artificial dissipation is added both to the right- and left-hand sides of the equations. To make the solution process economical, the left-hand side flux Jacobian terms are diagonalized, forming a set of scalar pentadiagonal equations that is solved by a backward Euler, alternating direction implicit procedure as developed by Pulliam (1984). The PARC code has the capability to calculate flow in a multiple-block domain. That capability was used extensively in the current study.

The algebraic turbulence model developed by Baldwin and Lomax (1978) was used in the present study. The model was applied globally, and no type of laminar-to-turbulent transition model was used, i.e., the flow was assumed to be fully turbulent everywhere. The search for the maximum of the Baldwin-Lomax model function "F" was stopped at a grid index approximately corresponding to the boundary-layer edge. The unit Reynolds number at the cascade face was 7.8×10^6 m^{-1}.

3.2. Computational Domain and Grids

The location of the computational domain had to be decided upon before proceeding with the calculations. The computational inlet was chosen to be a plane just downstream of an 8:1 streamwise contraction (referring to Fig. 1, a y-z plane at $x = 0$). Because of the strong acceleration caused by the contraction, boundary-layer growth was suppressed, so the flow was assumed to be uniform and one-dimensional over this plane. The computational exit was chosen to be a plane 2.2 cm (0.18 C_x) upstream of the blade leading edges, coincident with the measurement plane shown in Fig. 2, but extending to both inlet boards. This plane was chosen because endwall static pressure measurements were available to specify an exit flow condition as needed by the code. Some implications of this exit plane choice will be discussed with the computational results. Note that in Fig. 1 the spanwise thickness is uniform in the chosen computational domain and thus the geometry is symmetric about a plane through midspan. This fact was exploited to allow modeling of just half of the span.

With the computational boundaries chosen, the domain was discretized with grids that would allow for resolution of the necessary flow physics. The computational grid that was used for calculation of the original geometry is shown in Figure 3. This grid will be discussed here as an example; subsequent calculations of modified geometries used similar grids. Grid dimensions were chosen to be large enough to resolve the pertinent physics. Three separate grid blocks were chosen to cover the computational domain. The first two blocks are C-grids surrounding the upper and lower inlet boards. The C-grids were chosen to give good resolution of the inlet board's leading edges, which were suspected to be a possible source of the flow non-uniformity. An H-grid was used in the region between the C-grids and the computational inlet, overlapping the C-grids by several points. The dimensions of the three grids are shown in Fig. 3, with dimensions listed as the number of points streamwise, pitchwise, and spanwise. The total number of grid points for this calculation was 688,000, but because the PARC code computes each grid block independently, computer memory requirements are dictated by the size of the largest single grid block. Less than 8.0 M-words of core memory were required on a Cray Y-MP.

The fact that the computational domain was of constant spanwise cross-section simplified the grid generation process; two-dimensional grids were generated and then were stacked in the spanwise direction with a hyperbolic tangent stretching function. Fine grid spacing was used near all solid walls to resolve viscous layers. The location of the point adjacent to solid walls was specified such that $y^+ \lesssim 10$.

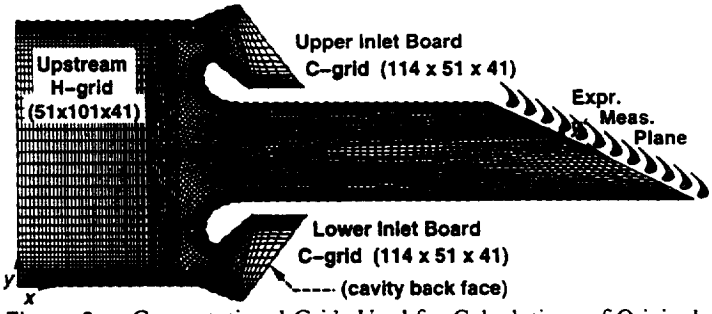

Figure 3. Computational Grids Used for Calculations of Original Geometry.

3.3. Boundary Conditions

Total conditions $P'_{in} = 96.94$ kPa (14.06 psi) and $T'_{in} = 294$ K (530°R) were specified at the computational inlet, and velocity components v and w were set to zero. Static conditions and the u-velocity component were then determined from characteristic information extrapolated from inside the domain. The symmetry plane was treated as an inviscid wall with no flux in the z-direction. All solid walls were treated as no-slip, adiabatic boundaries except the boundaries on the back face of the cavity. Resolving viscous layers on the back faces was not felt to be necessary because the flow in this region is nearly stagnant and thus more detailed modeling of the back faces would not affect the flow in the main passage. The cavity back faces were then treated as inviscid walls with zero flux. Because the exit flow is subsonic for all of the cases examined here, static pressure was specified at the exit and all other flow variables were extrapolated. More details of the exit flow condition will be discussed with the computational results.

4. DISCUSSION OF RESULTS

4.1. Calculation of Original Inlet Geometry

The grid shown in Fig. 3 was used for calculations of this case. Initially, a uniform exit static pressure, P_{ex}, was specified at the computational exit. The value of P_{ex} was obtained by averaging the measurements of endwall static pressure taps that were located in the same plane as the computational exit. Because this plane was located only 0.18 C_x upstream of the blade's leading edges, the pressure varied periodically between the blades. Using the average of the measurements was felt to be adequate for the current calculation because it would set up the correct mass flow and because whatever was creating the distortion had to have been generated sufficiently far upstream of the exit plane. The average

value of pressure was specified to be $P_{ex}/P'_{in} = 0.904$, which resulted in a total mass flow through the facility of 13.4 kg/s (29.5 lb/s). This was within 1% of the experimentally measured mass flow. The inlet freestream velocity and Mach number were $u_{in} = 44.7$ m/s and $M_{in} = 0.130$; computed exit values were $u_{ex} = 130.5$ m/s and $M_{ex} = 0.385$.

Starting the computational solution process proved to be difficult for this case. Originally, a uniform flow field of $M = 0.1$ was specified as an initial condition. The solution could not be advanced more than a few iterations before becoming numerically unstable. Therefore, a two-dimensional, midspan solution was obtained in an x-y plane and was stacked spanwise for use as an initial condition for the 3-D calculations.

Convergence of the solution was slow for this case, probably due to the relatively low Mach number flow regions and the flow recirculation in the cavities. The code was run in steps of 200 iterations, each run taking about one hour of CPU time. After 5000 iterations, the L_2 norm of the residuals leveled out after decreasing only by about 1.5 orders of magnitude. No evidence of total pressure distortions in the center of the passage was seen after 5000 steps, but the flow field still appeared to be changing. It appeared to stop changing after about 7500 steps but was run out to 8700 steps for added assurance. The overall inlet-to-exit mass flux error was less than 1%. Figure 4 shows results on the exit plane (looking downstream) obtained after 8700 steps. The contour plot of vorticity in that figure clearly shows a pair of streamwise vortices near $y' = 0.1$ inside the measurement plane and near $y' = 3.2$ outside the measurement plane. The total pressure contour plot shows, however, that while the vortices clearly distorted the flow, they were not strong enough to adversely affect the flow to the degree that was measured and shown in Fig. 2. The 0.8 and 0.9 contour lines did not turn over on themselves as the experimental data showed.

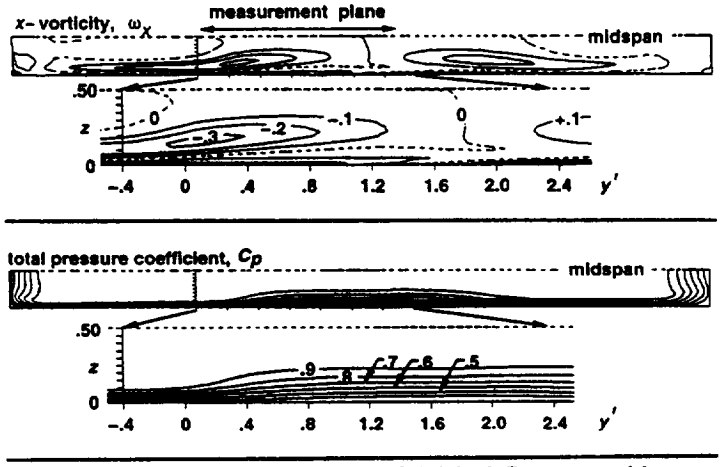

Figure 4. Results of Calculations of Original Geometry with Uniform Exit Static Pressure.

Recall that the computational exit plane was specified to be just 2.2 cm (0.18 C_x) upstream of the blade's leading edge plane. The effect of the blades is to provide an inlet flow blockage, accelerating the flow in the passages and decelerating it near the leading edges. This local acceleration could be expected to have a significant effect on the pair of vortices in the center of the passage. Accelerating flow stretches and strengthens streamwise vorticity, which would logically produce a higher degree of total pressure distortions. A more realistic exit static pressure distribution was therefore needed to account for blade blockage effects.

Endwall static pressure measurements were available on the computational exit plane, but the data was spatially quite coarse, with most blade passages having only one pressure tap. Fortunately, a three-dimensional Navier-Stokes CFD solution had previously been obtained for flow around a single blade in an infinite cascade. These results were obtained with the RVC3D code described by Chima (1992) and Chima and Yokota (1990). The single-blade calculations were run at the design inlet flow angle, $\alpha_{in} = 63.64°$, a Reynolds number of $Re_{C_x} = 0.497 \times 10^6$, and a subsonic exit Mach number of $M_{exit} = 0.9$. The inlet Mach number of 0.385, however, matches the exit Mach number that was used for calculations of the inlet geometry. A comparison of computational and experimental blade static pressure loading data is shown in Figure 5. The calculations were made of the full blade span and assume asymmetric inlet boundary layer thicknesses on the hub and tip endwalls. The comparison shows that the static pressure field is quite insensitive to the inlet boundary layer thickness and that the agreement between calculations and experiments is excellent. Given this excellent loading agreement, no inlet problem would have been suspected if not for the full pitchwise and spanwise inlet total pressure surveys. The loading diagrams also show that the flow in the blade passages is highly three-dimensional.

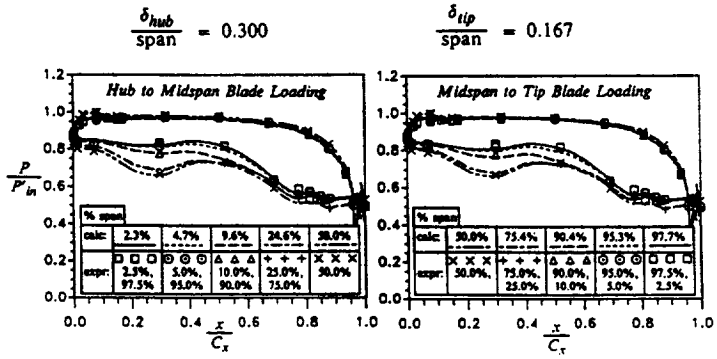

Figure 5. Blade Static Pressure Loading.

With the computational and experimental data giving confidence in the single blade calculations, computed static pressure values upstream of the blade row were interpolated onto a y'-z plane at a distance upstream of the blade's leading edges corresponding to the outflow plane of the inlet calculation. This single-blade interpolated field was then repeated 11 times to cover the entire computational exit plane. Finally, this pressure field had to be interpolated onto the outflow boundary grid of the present calculations. Figure 6 shows the exit static pressure distribution at various stages of interpolation. Note from this figure that the exit grid is rather coarse near the middle of the inlet section, which degrades the interpolation accuracy. For the purposes of determining the cause of the flow non-uniformity, however, this degree of accuracy was assumed to be sufficient.

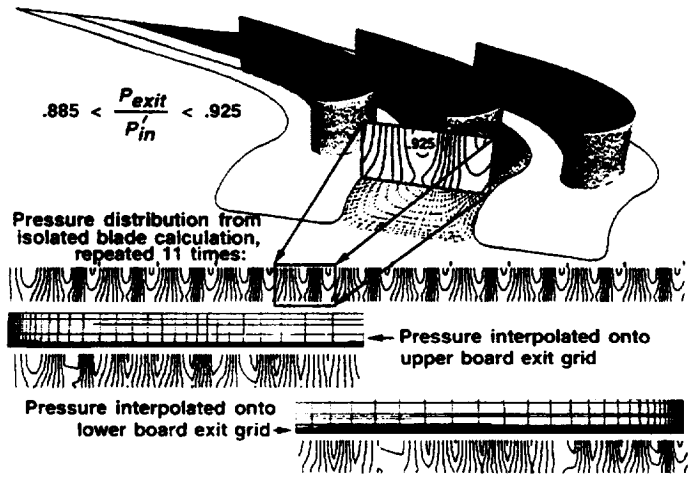

Figure 6. Non-uniform Static Pressure Distribution Used for Exit Condition.

Figure 7 shows results of the calculations with the non-uniform exit static pressure distribution. As expected, the blade blockage locally accelerated the flow, which strengthened the streamwise vortices. In comparing the total pressure measurements in Fig. 2 with the corresponding calculated results in Figs. 4 and 7, it is shown that this strengthening resulted in total pressure distortions consistent in strength and location to experimental measurements. The vortices are strong enough and sufficiently close to the endwall to cause cross-stream separation, resulting in rapid growth of the low total pressure regions. The behavior and effects of the streamwise vorticity on the total pressure profiles were similar to those observed by Harvey and Perry (1971), who experimentally studied the effects of trailing vortices in the vicinity of the ground. Ideal vortical flow theory (see, for example, Acheson, 1990) can be used to show that the vortices move slowly towards each other and lift off the endwall as they proceed downstream.

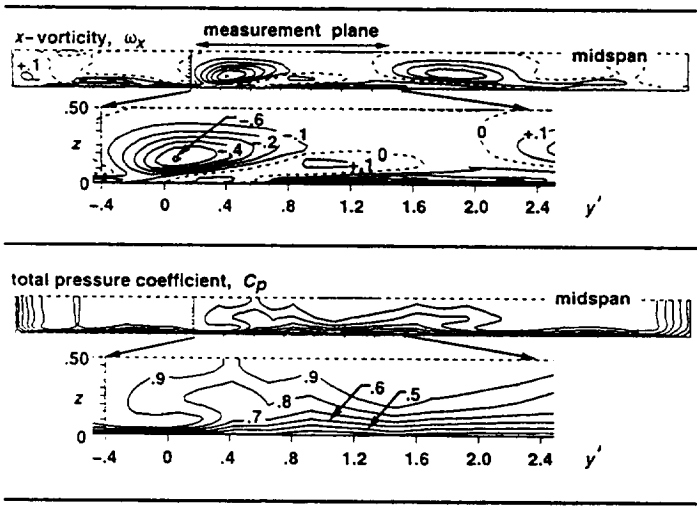

Figure 7. Results of Calculations of Original Geometry with Non-uniform Exit Static Pressure Distribution.

4.2. Analysis of Computed Flow

With excellent agreement at the measurement plane, the task was now to identify the upstream source of undesirable streamwise vortices and to determine how to eliminate them. The solution was analyzed to determine the source of the vortices by releasing "particles" into the computed flow field. Some of these particle traces, along with total pressure coefficient contours, are shown in Figure 8. The following discussion focuses on the lower inlet board cavity, but similar arguments apply for the upper one. As flow enters the inlet section, a low momentum boundary layer develops on the endwall because of the endwall viscous effects. Flow above the endwall boundary layer has significantly more momentum, allowing it to enter the cavity, thus forcing flow to exit the cavity near the endwall. With flow therefore passing over both sides of the inlet board's blunt leading edge, a horseshoe vortex forms near the leading edge/endwall junction. The passage side (as opposed to the cavity side) leg of this vortex is then convected in the y-direction by flow exiting the cavity near the endwall. With the primary flow in this area being essentially axial, the vortex is strengthened by strong z-directional shear caused by viscous effects of the endwall. The main flow then drives the vortex axially, directing it down the center of the passage, where it causes the total pressure distortions described above. Other interesting vortical flow phenomena is evident in Figs. 7 and 8, but will not be examined here as it is beyond the scope of this investigation.

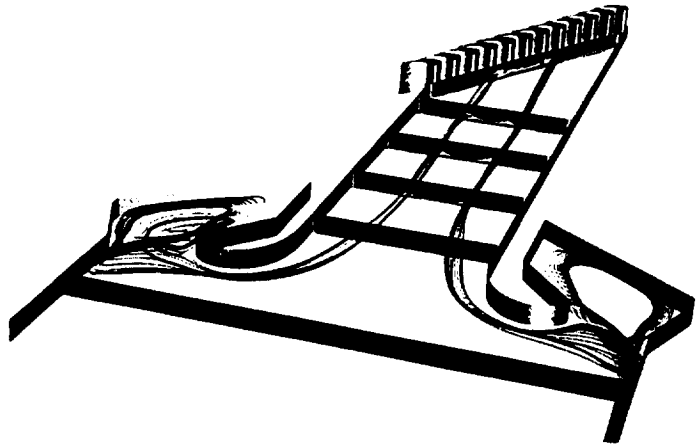

Figure 8. Particle Traces and Total Pressure Coefficient Contours.

4.3. Calculation of Modified Inlet Geometry

With the first objective of identifying the source of the flow non-uniformity met, the task of proposing a design change that would eliminate it was undertaken. A related experimental study of a vortex formed in the cavity of a two-dimensional submerged inlet was performed by Fleeger (1971). The strength of the cavity vortex was measured by paddle-type vortex meters and the effects of several geometric parameters were examined. The flow was modified in numerous ways: by inserting blocks to reduce the cavity width and height, by placing honeycomb material in the cavity, by adding corner fillets to the cavity, and by bleeding off the incoming boundary layers. The results showed that inserting honeycomb material or decreasing the depth of the cavity decreased the vortex formation. Rivir (1992) recommended eliminating the cavity and keeping the angle between the back face and the freestream velocity vector less than 70° to 80° to eliminate the vortex.

Another design change that was considered was to bleed air from the backs of the cavities to prevent any flow from exiting through their front face. This would, however, still allow horseshoe vortices to be set up in front of the inlet board's blunt leading edges as y-directional vortex lines wrap around them. The more acceptable design change was felt to be one in which the cavities, and thus the imbedded bellmouth nozzle, were completely eliminated.

The proposed new geometry and computational grids are shown in Figure 9. For comparison, an outline of the original geometry is included. The imbedded bellmouths were eliminated by bridging the cavities with straight boards attached to the upstream walls and to the original bellmouth nozzles. Two H-grid blocks were used for this calculation, each having 114 streamwise points, 51 points between the inlet boards, and 41 spanwise points, for a total of 477,000 grid points. The grids between the inlet boards and near the computational exit are identical to those used for the original geometry. Inlet and exit flow conditions and boundary conditions are identical as well. The non-uniform exit static pressure boundary condition was used.

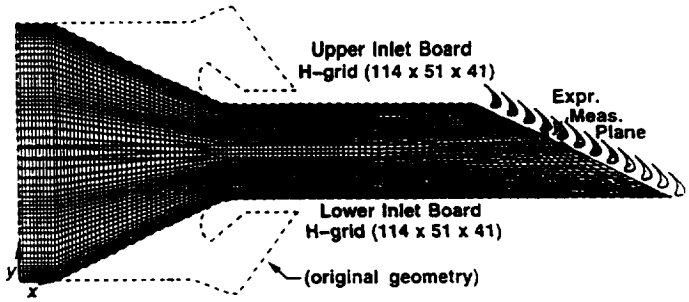

Figure 9. Computational Grids Used for Calculations of Modified Geometry.

Perhaps an early indicator of improved flow, it was found to be possible to start this solution with a uniform initial condition of $M = 0.1$, and a stacked 2-D solution was not necessary. Numerical convergence also proved to be more satisfactory for this case, with the L_2 residual norm decreasing by 3 orders of magnitude, although taking nearly 12,000 steps. About 350 steps were possible in each one CPU hour run. The overall inlet-to-exit mass flux error was less than 0.5%.

The vorticity and total pressure coefficient contour plots in Figure 10 show greatly improved flow conditions. Only small, weak vortices are seen near the corners, and they are of the opposite sense to those of the original geometry. As such, the vortices have no adverse effects on the flow near the center of the passage. This analysis clearly indicates that eliminating the imbedded bellmouth eliminates the pair of vortices, resulting in a flow with much greater pitchwise uniformity. Some small peaks of total pressure are seen in Fig. 10, but they are caused by the relatively coarse grid near the center of the passage and the resulting interpolation of the exit static pressure distribution.

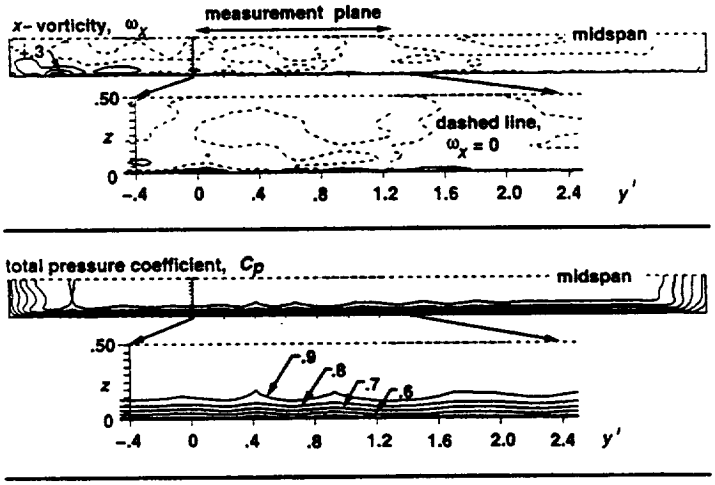

Figure 10. Results of Calculations of Modified Geometry with Non-uniform Exit Static Pressure Distribution.

4.4. Calculation of Modified Inlet Geometry with Upstream 8:1 Contraction

The original problem of pitchwise nonperiodic flow was clearly traced to the cavities formed by the imbedded bellmouth nozzles. Elimination of the cavities resulted in the elimination of the flow non-uniformity. Recall, however, that a rectangular-to-rectangular, 8:1 converging duct exists upstream of the constant span section (item K in Fig. 1). The 90° corners in this converging duct can be expected to produce some streamwise vorticity that may have an adverse effect on the downstream flow. Any vortices that were generated in corners of the contraction section with the original configuration probably would have been masked by the vortices generated in the cavities. However, with the cavities eliminated, these corner vortices could cause flow distortions.

Initially, calculations were run of the 8:1 contraction section isolated from the remainder of the modified inlet section. Because of symmetry in the y- and z-directions, only one quarter of the contraction had to be modeled. The geometry and grid for this calculation are shown in Figure 11. The same inlet conditions that were used for the other calculations were specified at the inlet of the contraction. In order to match the overall mass flux, the exit static pressure was specified to be $P_{ex}/P'_{in} = 0.989$, giving $M_{in} = 0.016$ and $M_{ex} = 0.125$. Despite the low Mach number conditions, convergence of the solution was good, with the L_2 residual norm dropping more than four orders of magnitude, and the inlet-to-exit mass flux error dropping to less than 0.05%, although taking 14,000 time steps to do so.

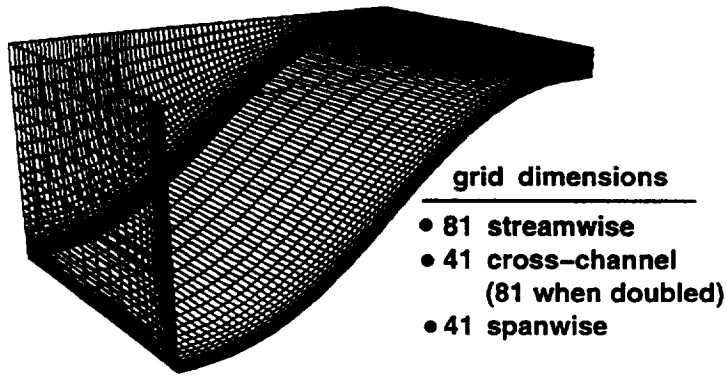

Figure 11. Computational Grid Used for Calculation of Upstream 8:1 Contraction Section.

Contours of streamwise vorticity and total pressure ratio are shown in Figure 12. The figure shows that streamwise vortices are generated in the corner, but that their impact on the total pressure field is minimal. Note, however, that the sense of the vortex is the same as the sense of the vortex that was generated in the cavity of the original geometry. To ensure that these vortices would not migrate to the center of the inlet, the contraction geometry was coupled to the modified inlet geometry and the flow was recalculated. The results at the exit plane of this calculation are the same as those shown in Fig. 10, and will thus not be repeated. Although streamwise vortices are indeed generated in the corners of the contraction, they are not convected to the center of the inlet and thus they have no detrimental effect on the flow at the cascade face.

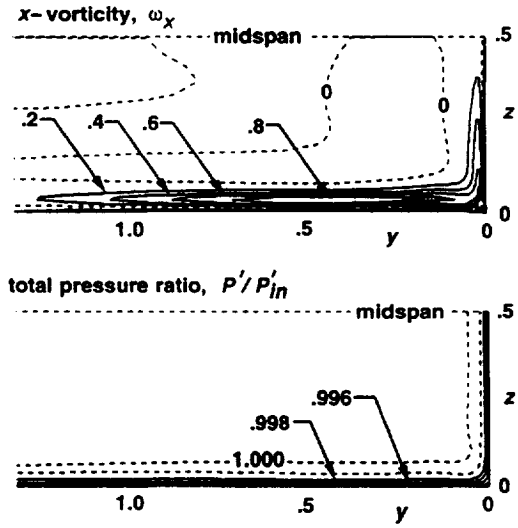

Figure 12. Results of Calculations of Upstream 8:1 Contraction Section.

4.5. Experimental Measurements of the Modified Inlet Geometry

With reasonable confidence that the distortion could be eliminated, the experimental hardware was modified to match the geometry shown in Fig. 9. A drawing of the actual hardware is shown in Figure 13. Note that the hardware is somewhat more complex than the original geometry shown in Fig. 1. Hinges were added between the original, horizontal inlet boards and the new inlet board sections to accommodate disk rotation. The hinges create a forward-facing step, but were designed and fabricated with a step height less than 1.0 mm (0.040 inches). Also, two new hinged lead screws were added to the new inlet board sections near the upstream attachment points.

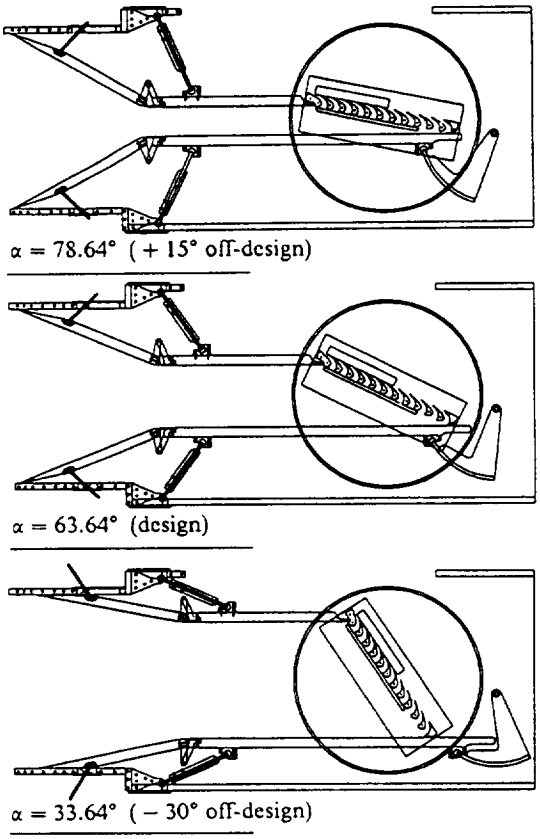

Figure 13. Transonic Turbine Blade Cascade - Modified Inlet Geometry.

Total pressure measurements were taken upstream of the blade's leading edges, on the same y'-z plane that was shown in Figs. 2, 4, 7, and 10. The results of the measurements from the modified geometry are presented in Figure 14. The measurements show good agreement with the calculations shown in Fig. 10. Most importantly, the measurements clearly show that the inlet flow distortion has been eliminated and that the flow upstream of the blades is pitchwise periodic and two-dimensional, as was initially desired.

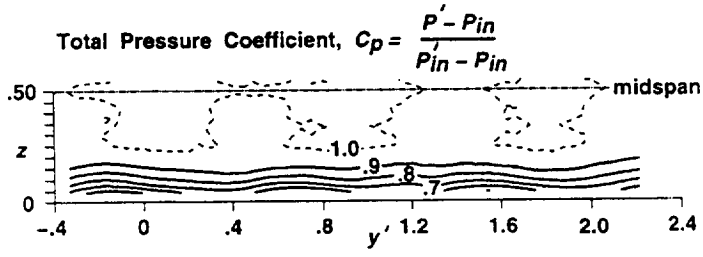

Figure 14. Experimental Measurements of Total Pressure Coefficient in the Modified Geometry.

5. SUMMARY AND CONCLUSIONS

The results indicate that the CFD analysis was quite successful in aiding in the redesign of the cascade inlet. Calculations of the original geometry showed total pressure loss regions consistent in strength and location to the experimental measurements. The calculations further showed that these loss regions were caused by a pair of streamwise vortices that originated as a result of the interaction of the flow with cavities formed by the bellmouth inlet. With the origin of the distortions well understood, calculations were performed on a geometry that eliminated the cavities by bridging the region between the bellmouth inlet and the upstream wall. These calculations showed that eliminating the cavities successfully eliminated the flow distortions at the cascade face. Additional calculations showed that streamwise vortices generated in the corners of the upstream 8:1 contraction section have no detrimental effect on the flow uniformity at the cascade face.

This study exemplifies the use of CFD as a diagnostic and a design tool. It also exemplifies the inherent coupling of computational, analytical, and experimental fluid dynamics and heat transfer. Moreover, the study shows that a detailed analysis of an entire facility may be necessary in order to obtain benchmark quality data. That data can then, in turn, be used more reliably to aid in the improvement of CFD models and codes.

ACKNOWLEDGEMENTS

This work was supported by the NASA Lewis Research Center under contract NAS3-25266 with Sverdrup Technology, Inc. and contract NAS3-27186 with NYMA, Inc., both with Mr. Robert J. Boyle as monitor.

REFERENCES

Acheson, D. J., 1990, *Elementary Fluid Dynamics*, Clarendon Press, Oxford, U.K., pp. 128-129, 177-178.

Baldwin, B. S., and Lomax, H., 1978, "Thin-Layer Approximation and Algebraic Model for Separated Turbulent Flows," AIAA Paper No. 78-257.

Chima, R. V., 1992, "Viscous Three-Dimensional Calculations of Transonic Fan Performance," in *CFD Techniques for Propulsion Applications*, AGARD Conference Proceedings No. CP-510, AGARD, Neuilly-Sur-Seine, France, pp. 21-1 to 21-19.

Chima, R. V., and Yokota, J. W., 1990, "Numerical Analysis of Three-Dimensional Viscous Internal Flows," *AIAA J.*, Vol. 28, No. 5, pp. 798-806.

Cooper, G. K., and Sirbaugh, J. R., 1989, "PARC Code: Theory and Usage," AEDC-TR-89-15.

Fleeger, D. W., 1971, "Investigation of a Vortex in the Inlet of a Submerged Nozzle," M.S. Thesis, Air Force Institute of Technology, Wright-Patterson Air Force Base, OH.

Fottner, L., ed., 1990, "Test Cases for Computation of Internal Flow in Aero Engine Components," prepared by the Propulsion and Energetics Panel Working Group 18, AGARD Advisory Report No. 275.

Harvey, J. K., and Perry, F. J., 1971, "Flowfield Produced by Trailing Vortices in the Vicinity of the Ground," *AIAA J.*, Vol. 9, No. 8, pp. 1659-1660.

Kiock, R., Lehthaus, F., Baines, N. C., Sieverding, C. H., 1985, "The Transonic Flow Through a Plane Turbine Cascade as Measured in Four European Wind Tunnels," ASME Paper No. 85-IGT-44.

Kline, J. F., Moffitt, T. P., and Stabe, R. G., 1983, "Incidence Loss for Fan Turbine Rotor Blade in Two-Dimensional Cascade," NASA TP-2188.

Meauze, G. 1979, "Transonic Boundary Layer on Compressor Stator Blades as Calculated and Measured in Wind Tunnel," 44th International Symposium on Air Breathing Engines, ISABE, Orlando, Florida, April 1-6, 1979.

Pulliam, T.H., 1984, "Euler and Thin Layer Navier-Stokes Codes: ARC2D, ARC3D," in *Notes for Computational Fluid Dynamics User's Workshop*, The University of Tennessee Space Institute, Tullahoma, Tennessee, UTSI Publication E02-4005-023-84, March 12-16, pp. 15.1-15.85.

Rivir, R. B., 1992, *Private Communication.*

Stabe, R. G., and Kline, J. F., 1974, "Incidence Loss for a Core Turbine Rotor Blade in a Two-Dimensional Cascade," NASA TM-X-3047.

Verhoff, V. G., Camperchioli, W. P., and Lopez, I., 1992, "Transonic Turbine Blade Cascade Testing Facility," AIAA Paper No. 92-4034, NASA TM-105646.

REPORT DOCUMENTATION PAGE

Form Approved
OMB No. 0704-0188

1. AGENCY USE ONLY (*Leave blank*)	2. REPORT DATE	3. REPORT TYPE AND DATES COVERED
	July 1996	Technical Memorandum

4. TITLE AND SUBTITLE

Three-Dimensional Navier-Stokes Analysis and Redesign of an Imbedded Bellmouth Nozzle in a Turbine Cascade Inlet Section

5. FUNDING NUMBERS

WU–505–62–10

6. AUTHOR(S)

P.W. Giel, J.R. Sirbaugh, I. Lopez, and G.J. Van Fossen

7. PERFORMING ORGANIZATION NAME(S) AND ADDRESS(ES)

NASA Lewis Research Center
Cleveland, Ohio 44135–3191
and
Vehicle Propulsion Directorate
U.S. Army Research Laboratory
Cleveland, Ohio 44135–3191

8. PERFORMING ORGANIZATION REPORT NUMBER

E–10359

9. SPONSORING/MONITORING AGENCY NAME(S) AND ADDRESS(ES)

National Aeronautics and Space Administration
Washington, D.C. 20546–0001
and
U.S. Army Research Laboratory
Adelphi, Maryland 20783–1145

10. SPONSORING/MONITORING AGENCY REPORT NUMBER

NASA TM–107284
ARL–MR–152

11. SUPPLEMENTARY NOTES

Prepared for the 39th International Gas Turbine and Aeroengine Congress and Exposition sponsored by the American Society of Mechanical Engineers, The Hague, Netherlands, June 13–16, 1994. P.W. Giel and J.R. Sirbaugh, NYMA, Inc., 2001 Aerospace Parkway, Brook Park, Ohio 44142 (work performed under NASA Contract NAS3–27186); I. Lopez, Vehicle Propulsion Directorate, U.S. Army Research Laboratory, NASA Lewis Research Center; G.J. Van Fossen, NASA Lewis Research Center. Responsible person, G.J. Van Fossen, organization code 2630, (216) 433–5892.

12a. DISTRIBUTION/AVAILABILITY STATEMENT

Unclassified - Unlimited
Subject Categories 34, 02, 07, and 09

This publication is available from the NASA Center for AeroSpace Information, (301) 621–0390.

12b. DISTRIBUTION CODE

13. ABSTRACT (*Maximum 200 words*)

Experimental measurements in the inlet of a transonic turbine blade cascade showed unacceptable pitchwise flow non-uniformity. A three-dimensional, Navier-Stokes computational fluid dynamics (CFD) analysis of the imbedded bellmouth inlet in the facility was performed to identify and eliminate the source of the flow non-uniformity. The blockage and acceleration effects of the blades were accounted for by specifying a periodic static pressure exit condition interpolated from a separate three-dimensional Navier-Stokes CFD solution of flow around a single blade in an infinite cascade. Calculations of the original inlet geometry showed total pressure loss regions consistent in strength and location to experimental measurements. The results indicate that the distortions were caused by a pair of streamwise vortices that originated as a result of the interaction of the flow with the imbedded bellmouth. Computations were performed for an inlet geometry which eliminated the imbedded bellmouth by bridging the region between it and the upstream wall. This analysis indicated that eliminating the imbedded bellmouth nozzle also eliminates the pair of vortices, resulting in a flow with much greater pitchwise uniformity. Measurements taken with an installed redesigned inlet verify that the flow non-uniformity has indeed been eliminated.

14. SUBJECT TERMS

Duct geometry; Cascade flow; Fluid dynamics; Three-dimensional flow; Computational fluid dynamics

15. NUMBER OF PAGES

10

16. PRICE CODE

A02

17. SECURITY CLASSIFICATION OF REPORT	18. SECURITY CLASSIFICATION OF THIS PAGE	19. SECURITY CLASSIFICATION OF ABSTRACT	20. LIMITATION OF ABSTRACT
Unclassified	Unclassified	Unclassified	

National Aeronautics and
Space Administration

Lewis Research Center
21000 Brookpark Rd.
Cleveland, OH 44135-3191